Int. J. Solids Structures, 1967, Vol. 3, pp. 657 to 675. Pergamon Press Ltd. Printed in Great Britain

AXIALLY SYMMETRIC WAVE PROPAGATION IN A TWO-LAYERED CYLINDER*

J. S. WHITTIER and J. P. JONES

Aerospace Corporation, El Segundo, California

Abstract—The linear theory of elasticity is used to investigate axially symmetric wave propagation in an infinitely long two-layered cylinder. Each material is taken to be homogeneous and isotropic. A perfect bond is assumed at the interface, while the inner and outer boundaries of the composite cylinder are treated as traction-free. The dispersion determinant relating phase velocity and wave number for a harmonic train of waves satisfying these boundary conditions is presented. The character of the dispersion equation is investigated analytically and numerically. Stress and displacement distributions are also presented for the numerical example. Comparisons are made with an approximate solution of the same problem obtained by means of a thin shell theory incorporating thickness-shear deformation of each layer.

NOTATION

a	radius of the interface
A, B, C, D	arbitrary constants
c	phase velocity, ω/k
E	Young's modulus
H	h_1+h_2
h_1, h_2	thickness of outer and inner layer, respectively
i	$+\sqrt{-1}$
I_0, K_0, I_1, K_1	modified Bessel functions of the first and second kind
J_0, N_0, J_1, N_1	Bessel functions of the first and second kind
k	wave number
$P_{ij}, Q_{ij}, R_{ij}, S_{ij}$, $T_{ij}, U_{ij}, V_{ij}, W_{ij}$	see Appendix
r, θ, z	cylindrical coordinates
s	c/β^*
t	time
u_r, u_θ, w	displacements in cylindrical coordinates
α^2	$(\lambda+2\mu)/\rho$
β^2	μ/ρ
ε_i, δ_i	See equation (9)
Δ	kH
λ, μ	Lamé's elastic constants
λ_1, λ_2	$h_1/a, h_2/a$
ν	Poisson's ratio
ρ	density
$\sigma_{rr}, \sigma_{rz}, \sigma_{zz}$	stress components
ϕ	dilatational potential
Ψ	equivoluminal potential
ω	frequency
Ω	$\omega H/\beta^*$
β^*	$(\beta_1+\beta_2)/2$

1. INTRODUCTION

IN recent years considerable attention has been focused on multilayered shells. Often a sandwich-type construction is used to lighten the weight of a shell structure; in other

* This research was supported by the U.S. Air Force under Contract No. AF 04(695)-469.

instances, a protective layer is bonded to a shell as, for example, in the case of a re-entry vehicle heat shield or a rocket nozzle liner. Two-layered thick shell configurations are also used in solid propellant rocket motors.

This study employs the linear theory of elasticity and treats the propagation of a train of waves in an infinitely long, two-layered cylinder; each layer is homogeneous and isotropic. Computations based on this solution are used in an assessment of the accuracy of an approximate two-layered shell theory that was presented recently [1]. This latter theory included the effects of shear deformation and rotatory inertia.* In [1], a partial comparison is made between the shell theory and the solutions obtained in the present work using the linear theory of elasticity. Dispersion curves were compared in detail, and a few displacement distribution comparisons were made. The present work gives detailed displacement comparisons over a larger frequency and wave number regime and also presents stress distribution comparisons.

The propagation of waves in cylindrically bounded media has been extensively investigated. Although most of the work has been limited to cylinders of a single material, it is of interest to recall a few of the more pertinent references. Pochhammer [2] and Chree [3] first formulated the problem for solid cylindrical bars. Ghosh [4] formulated the problem for hollow cylindrical bars but presented no calculations. Later, Gazis [5–7] and Greenspon [8, 9] made extensive numerical calculations for the vibrations of a hollow cylinder and compared them with several approximate shell theories such as those of Herrmann and Mirsky [10–12] and Naghdi and Cooper [13, 14]. Other investigators include Bird [15] and Bird *et al.* [16].

The vibrations of a multilayered cylinder using the equations of the linear theory of elasticity have not been extensively investigated. Baltrukonis *et al.* [17] treated simple thickness-shear vibrations of a two-layered cylinder, and McNiven *et al.* [18] treated propagation of axially symmetric waves in solid bars with an outer finite layer. Other than these, the authors know of no other references treating multilayered cylinders by the linear theory of elasticity.

Layered half-planes have been extensively treated by geophysicists [19], but their work is not particularly of interest here since geophysical earth models always have one infinite layer. Of the plane two medium problems with finite layers, the symmetrical sandwich two-dimensional beam is treated by Saito and Sato [20], and the asymmetrical two-layered counterpart is treated by Jones [21]. The last reference is especially *apropos* since it is shown here that the wave propagation solution of the two-layered cylinder problem degenerates into the solution of the plane two layered medium problem when the wavelength becomes sufficiently small compared to the thickness.

The present analysis is formulated in terms of displacement potentials. A solution in the form of an infinite train of axially symmetric waves is assumed. To satisfy boundary conditions the phase velocity (or frequency) must depend on wave number in such a way that an eighth-order determinant vanishes. Due to its complexity little analytical progress can be made with this dispersion determinant except in special cases. However, for infinitely long waves the determinant reduces to a product of two fourth-order determinants whose frequency roots correspond to vibrations with either purely axial or purely radial motion. Alternatively, for very short waves the determinant reduces to a form given previously by Jones [21] for a plane two-layered medium. Here the phase velocity roots correspond to

* For a more extensive bibliography dealing with the thin shell literature of layered shells see [1].

Rayleigh waves on the free surfaces and a possible Stoneley wave at the interface.* For waves of intermediate length, roots of the dispersion determinant are found numerically with a digital computer program described herein. Displacement and stress distributions corresponding to these roots are also found for a specific numerical example, and these are used to estimate the accuracy of the previously mentioned shell theory.

It is concluded that a Timoshenko-type shell theory gives good agreement with the present exact solution in a region of applicability encompassing low enough frequencies and large enough wavelengths. It appears that to extend this region of applicability one must use a shell theory incorporating thickness-stretch motion. On the basis of the displacements obtained from the exact theory, a linear distribution of radial motion does not appear to be an unreasonable first approximation for a thickness-stretch theory.

2. ANALYSIS

Consider a doubly infinite hollow cylinder composed of two homogeneous, isotropic, elastic media with Lamé constants λ_1, μ_1, λ_2, and μ_2 and densities ρ_1 and ρ_2, where subscript 1 refers to the outer layer and subscript 2 refers to the inner layer. The cylinders are perfectly bonded together at the interface. Cylindrical coordinates r, θ, and z are employed. The interface radius is denoted by a, and the thicknesses are h_1 and h_2.

Written in terms of the potential functions ϕ and Ψ the equations of elasticity for motions with torsionless axial symmetry are

$$\nabla^2\phi = \frac{1}{\alpha^2}\phi_{,tt}, \qquad \nabla^2\Psi = \frac{1}{\beta^2}\Psi_{,tt} \tag{1}$$

where the displacements and stresses may be generated from the potential functions by

$$u_\theta = 0, \qquad u_r = \phi_{,r} + \Psi_{,rz}, \qquad w = \phi_{,z} - \frac{1}{r}(r\Psi_{,r})_{,r} \tag{2}$$

$$\sigma_{rr} = \lambda\left(\frac{1}{r}\phi_{,r} + \phi_{,rr} + \phi_{,rz}\right) + 2\mu(\phi_{,r} + \Psi_{,rz})_{,r} \tag{3}$$

$$\sigma_{rz} = \mu\left(2\phi_{,rz} + \Psi_{,zz} - \Psi_{,rr} - \frac{1}{r}\Psi_{,r}\right)_{,r} \tag{4}$$

$$\sigma_{zz} = \lambda\left(\frac{1}{r}\phi_{,r} + \phi_{,rr} + \phi_{,zz}\right) + 2\mu\left[\phi_{,zz} - \frac{1}{r}(r\Psi_{,rz})_{,r}\right]. \tag{5}$$

The terms u and w are the radial and axial displacements, respectively, and σ_{rr}, σ_{rz}, and σ_{zz} are the stress components. The expression for $\sigma_{\theta\theta}$ is omitted since it is not essential to the problem. All other stress components are zero and α and β are the dilatational and equivoluminal wave speeds defined by

$$\alpha^2 = \frac{\lambda + 2\mu}{\rho}, \qquad \beta^2 = \frac{\mu}{\rho}. \tag{6}$$

* A Stoneley wave may or may not exist at an interface depending on the elastic properties and densities of the two media ([19], p. 113).

Equations (1–5) hold in either layer provided appropriate values of α, β, λ and μ are used.

If a Rayleigh train of waves is assumed, then all quantities are considered to vary as

$$w = \bar{w}(r)e^{i(kz-\omega t)}, \qquad \sigma_{rr} = \bar{\sigma}_{rr}(r)e^{i(kz-\omega t)}, \qquad \text{etc.} \tag{7}$$

and the solution to equations (1) is (the factor $e^{i(kz-\omega t)}$ has been suppressed for compactness)

$$\begin{aligned} \phi &= AI_0(k\varepsilon r)+BK_0(k\varepsilon r) \\ ik\Psi &= CI_0(k\delta r)+DK_0(k\delta r). \end{aligned} \tag{8}$$

Here I_0 and K_0 are modified Bessel functions of the first and second kind and zeroth order.* The solutions equation (8) hold in either medium provided the parameters appropriate to each medium are used in the equations. Thus there will be two sets of ε's and δ's:

$$\begin{aligned} \varepsilon_1^2 &= 1-\frac{c^2}{\alpha_1^2}, & \varepsilon_2^2 &= 1-\frac{c^2}{\alpha_2^2} \\ \delta_1^2 &= 1-\frac{c^2}{\beta_1^2}, & \delta_2^2 &= 1-\frac{c^2}{\beta_2^2} \end{aligned} \tag{9}$$

where

$$c^2 = \frac{\omega^2}{k^2}. \tag{10}$$

Also there will be two sets of constants A_1, A_2 and B_1, B_2, etc., to be determined by application of boundary conditions on σ_{rr}, σ_{rz}, u_r, and w. Expressing the displacements and stresses in terms of the solutions, equation (8), one obtains

$$\begin{aligned} \frac{\sigma_{rr}}{\mu} = k^2\left\{\left[A(1+\delta^2)I_0(k\varepsilon r)-2\varepsilon^2\frac{I_1(k\varepsilon r)}{k\varepsilon r}\right]+B\left[(1+\delta^2)K_0(k\varepsilon r)+2\varepsilon^2\frac{K_1(k\varepsilon r)}{k\varepsilon r}\right]\right\} \\ +2k^2\delta^2\left\{C\left[I_0(k\delta r)-\frac{I_1(k\delta r)}{k\delta r}\right]+D\left[K_0(k\delta r)+\frac{K_1(k\delta r)}{k\delta r}\right]\right\} \end{aligned} \tag{11}$$

$$\frac{\sigma_{rz}}{\mu} = 2ik^2\varepsilon[AI_1(k\varepsilon r)-BK_1(k\varepsilon r)]+ik^2\delta[C(1+\delta^2)I_1(k\delta r)-D(1+\delta^2)K_1(k\delta r)] \tag{12}$$

$$u_r = k[A\varepsilon I_1(k\varepsilon r)-B\varepsilon K_1(k\varepsilon r)+C\delta I_1(k\delta r)-D\delta K_1(k\delta r)] \tag{13}$$

$$w = ik[AI_0(k\varepsilon r)+BK_0(k\varepsilon r)+C\delta^2 I_0(k\delta r)+D\delta^2 K_0(k\delta r)]. \tag{14}$$

The above expressions are valid in each region provided appropriate values of A_i, B_i, C_i, D_i, ε_i, δ_i, $\mu_i (i = 1, 2)$ are used.

The boundary conditions for the free vibration problem are

* Obviously, when ε or δ are imaginary, the appropriate analytic continuations of the I and K functions must be used, as given in [24].

$$\left.\begin{aligned} &\sigma_{rr}^{(1)} = \sigma_{rz}^{(1)} = 0 \quad \text{at} \quad r = a+h_1 \\ &\sigma_{rr}^{(2)} = \sigma_{rz}^{(2)} = 0 \quad \text{at} \quad r = a-h_2 \end{aligned}\right\}$$

and

$$\left.\begin{aligned} \sigma_{rr}^{(1)} = \sigma_{rr}^{(2)}, \qquad \sigma_{rz}^{(1)} = \sigma_{rz}^{(2)}, \qquad u^{(1)} = u^{(2)} \\ w^{(1)} = w^{(2)} \quad \text{at} \quad r = a. \end{aligned}\right\} \tag{15}$$

The superscripts indicate quantities in medium 1 or 2. From the boundary condition, equation (15), one obtains with the aid of equations (11–14) eight linear homogeneous equations for the eight constants $A_1 \ldots D_2$. Since the equations are long and their formulations are straightforward, the equations are presented in the Appendix rather than in the text.

To assure nontrivial values of $A_1, B_1, \ldots, C_2, D_2$, the determinant of their coefficients must be set equal to zero. This constitutes the dispersion equation. The determinant is as shown in equation (16) on page 662: where, for brevity, the quantities $P_{11} \ldots W_{22}$ are expressions containing Bessel functions and are defined in the Appendix.

The determinant, equation (16), is so complicated that little can be done to obtain any general analytical results.* However, simpler forms of the determinant are obtainable for the limiting cases of very long and very short waves.

For infinite wavelengths, i.e., $k = 0$, the solutions, equation (8), become independent of z, and the determinant degenerates to the product of two fourth-order determinants. A more straightforward derivation of these fourth-order determinants involves repeating the calculations with the z dependence excluded from the outset. Then it is clear that one of the fourth-order determinants corresponds to purely radial motions while the other corresponds to purely axial motions.

Equating the radial motion determinant to zero one obtains the frequency equation for simple thickness-stretch vibrations as shown in equation (17) on page 663: where J_0, N_0, J_1, N_1 are Bessel functions of the first and second kinds of orders zero and one, respectively.

Equating the axial motion determinant to zero one obtains the frequency equation for axial shear vibrations

$$\begin{vmatrix} J_1\left[\frac{\omega}{\beta_1}(a+h_1)\right] & N_1\left[\frac{\omega}{\beta_1}(a+h_1)\right] & 0 & 0 \\ J_1\left(\frac{\omega}{\beta_1}a\right) & N_1\left(\frac{\omega}{\beta_1}a\right) & -\frac{\mu_2\beta_1}{\mu_1\beta_2}J_1\left(\frac{\omega}{\beta_2}a\right) & -\frac{\mu_2\beta_1}{\mu_1\beta_2}N_1\left(\frac{\omega}{\beta_2}a\right) \\ J_0\left(\frac{\omega}{\beta_1}a\right) & N_0\left(\frac{\omega}{\beta_1}a\right) & -J_0\left(\frac{\omega}{\beta_2}a\right) & -N_0\left(\frac{\omega}{\beta_2}a\right) \\ 0 & 0 & J_1\left[\frac{\omega}{\beta_2}(a-h_2)\right] & N_1\left[\frac{\omega}{\beta_2}(a-h_2)\right] \end{vmatrix} = 0. \tag{18}$$

Equation (18) has been obtained by Baltrukonis *et al.* [17].

* As was suggested by a referee, the frequency determinant equation (16) does not directly reduce to the frequency equation given in [18] due to the singular behavior of certain Bessel functions appearing in (16).

$$
\begin{vmatrix}
P_{11} & Q_{11} & R_{11} & S_{11} & 0 & 0 & 0 & 0 \\
T_{11} & -U_{11} & V_{11} & -W_{11} & 0 & 0 & 0 & 0 \\
\mu_1 P_{10} & \mu_1 Q_{10} & \mu_1 R_{10} & \mu_1 S_{10} & -\mu_2 P_{20} & -\mu_2 Q_{20} & -\mu_2 R_{20} & -\mu_2 S_{20} \\
\mu_1 T_{10} & -\mu_1 U_{10} & \mu_1 V_{10} & -\mu_1 W_{10} & -\mu_2 T_{20} & \mu_2 U_{20} & -\mu_2 V_{20} & \mu_2 W_{20} \\
\varepsilon_1 I_1(k\varepsilon_1 a) & -\varepsilon_1 K_1(k\varepsilon_1 a) & \delta_1 I_1(k\delta_1 a) & -\delta_1 K_1(k\delta_1 a) & -\varepsilon_2 I_1(k\varepsilon_2 a) & \varepsilon_2 K_1(k\varepsilon_2 a) & -\delta_2 I_1(k\delta_2 a) & \delta_2 K_1(k\delta_2 a) \\
I_0(k\varepsilon_1 a) & K_0(k\varepsilon_1 a) & \delta_1^2 I_0(k\delta_1 a) & \delta_1^2 K_0(k\delta_1 a) & -I_0(k\varepsilon_2 a) & -K_0(k\varepsilon_2 a) & -\delta_2^2 I_0(k\delta_2 a) & -\delta_2^2 K_0(k\delta_2 a) \\
0 & 0 & 0 & 0 & -P_{22} & -Q_{22} & -R_{22} & -S_{22} \\
0 & 0 & 0 & 0 & -T_{22} & U_{22} & -V_{22} & W_{22}
\end{vmatrix} = 0 \qquad (16)
$$

$$
\begin{vmatrix}
\frac{\omega\alpha_1}{\beta_1^2}J_0\left[\frac{\omega}{\alpha_1}(a+h_1)\right] & \frac{\omega\alpha_1}{\beta_1^2}N_0\left[\frac{\omega}{\alpha_1}(a+h_1)\right] & 0 & 0 \\
-\frac{2}{a+h_1}J_1\left[\frac{\omega}{\alpha_1}(a+h_1)\right] & -\frac{2}{a+h_1}N_1\left[\frac{\omega}{\alpha_1}(a+h_1)\right] & & \\
J_1\left(\frac{\omega a}{\alpha_1}\right) & N_1\left(\frac{\omega a}{\alpha_1}\right) & -J_1\left(\frac{\omega a}{\alpha_2}\right) & -N_1\left(\frac{\omega a}{\alpha_2}\right) \\
\frac{\omega\alpha_1}{\beta_1^2}J_0\left(\frac{\omega a}{\alpha_1}\right) & \frac{\omega\alpha_1}{\beta_1^2}N_0\left(\frac{\omega a}{\alpha_1}\right) & -\frac{\mu_2}{\mu_1}\left[\frac{\omega\alpha_2}{\beta_2^2}J_0\left(\frac{\omega a}{\alpha_2}\right)\right. & -\frac{\mu_2}{\mu_1}\left[\frac{\omega\alpha_2}{\beta_2^2}N_0\left(\frac{\omega a}{\alpha_2}\right)\right. \\
-\frac{2}{a}J_1\left(\frac{\omega a}{\alpha_1}\right) & -\frac{2}{a}N_1\left(\frac{\omega a}{\alpha_1}\right) & \left.-\frac{2}{a}J_1\left(\frac{\omega a}{\alpha_2}\right)\right] & \left.-\frac{2}{a}N_1\left(\frac{\omega a}{\alpha_2}\right)\right] \\
0 & 0 & \frac{\omega\alpha_2}{\beta_2^2}J_0\left[\frac{\omega}{\alpha_2}(a-h_2)\right] & \frac{\omega\alpha_2}{\beta_2^2}N_0\left[\frac{\omega}{\alpha_2}(a-h_2)\right] \\
 & & -\frac{2}{a-h_2}J_1\left[\frac{\omega}{\alpha_2}(a-h_2)\right] & -\frac{2}{a-h_2}N_1\left[\frac{\omega}{\alpha_2}(a-h_2)\right]
\end{vmatrix} = 0 \quad (17)
$$

For very short wavelengths compared to the interface radius of the cylinder, it would be expected that propagation of axially symmetric waves in a two-layered cylinder would differ very little from propagation of straight crested waves in a plane two-layered medium at least for a thin cylinder. The truth of this supposition can be shown analytically in equation (16) by replacing I_0, I_1, K_0, and K_1 by their asymptotic values for large arguments:

$$I_0, I_1(x) \cong \frac{e^x}{(2\pi x)^{\frac{1}{2}}}$$

$$K_0, K_1(x) = \left(\frac{\pi}{2x}\right)^{\frac{1}{2}} e^{-x} \tag{19}$$

$$(x \gg 1).$$

With these substitutions and a slight redefinition of coefficients in equations (A1–A8), the dispersion determinant becomes the same as that given by Jones [21] for the plane two-layered problem. As would be expected, the waves degenerate into two Rayleigh surface waves, one in each medium, and a possible Stoneley wave at the interface.

For wavelengths of intermediate size it is difficult to extract much information about the character of the possible wave propagation solutions except by considering specific numerical examples. This is done in the following section where the results of the numerical example are also used to check the accuracy of the shell theory given in [1].

3. COMPUTATIONS

In order to investigate the character of the wave propagation solutions governed by equations (A1–A8) numerical analysis was employed. A program for the IBM 7094 computer was developed at the Aerospace Corporation for determining phase velocities (and from them, frequencies) satisfying equation (16). To facilitate the use of the present solution for assessing the range of validity of approximate shell theories, displacement and stress distributions through the cylinder thickness are calculated as well.

For a given numerical problem valid computer results are obtained only for a limited range of wavelengths. The largest number available for routine calculation is $10^{38} \sim \exp(88)$, while for large wave numbers the I's (modified Bessel functions of the first kind) are of the order of $\exp[(kH)(a/H)]$. Here $H = h_1 + h_2$ is the total wall thickness of the cylinder. Thus, for valid computer results, kH cannot be much larger than $88(H/a)$. In the example to be considered here a/H is 30 so that $kH < 3$ gives a fair estimate of the range amenable to computations based on equation (16). For larger values of kH the wavelength is short compared to the radius of the cylinder, the asymptotic expressions of equation (19) are appropriate, and satisfactory numerical results are obtained using a computer program based on the plane medium equations of [21].

Due to the large number of parameters associated with this problem, a complete parametric study is beyond the scope of this work. Consequently, a specific numerical example was chosen for study: The numerical values are those which arose in connection with a study of vulnerability of a hypothetical reentry vehicle. Properties of the cylinder chosen for detailed numerical study are given in Table 1. This example was also used to check the validity of the approximate shell theory of [1] where dispersion curves were compared for low frequencies and large wavelengths. Dispersion curves are presented here for

the first nine modes of axially symmetric wave propagation. Distributions of displacements and stresses through the thickness of the cylinder are also presented, and for the first four modes these are compared with the distributions predicted by the approximate shell theory [1].

TABLE 1. NUMERICAL PROPERTIES OF THE CYLINDER STUDIED

Properties	Outer layer	Inner layer
Material constants	$E_1 = 4{\cdot}00 \quad 10^6$ lb/in^2 $\nu_1 = \frac{1}{4}$ $\rho_1 = \frac{0{\cdot}080}{386}$ lb-sec^2/in^4	$E_2 = 30{\cdot}0 \quad 10^6$ lb/in^2 $\nu_2 = \frac{1}{3}$ $\rho_2 = \frac{0{\cdot}286}{386}$ lb-sec^2/in^4
Geometrical parameters	$\frac{a}{H} = 30 \quad \frac{h_1}{H} = 0{\cdot}3 \quad \frac{h_2}{H} = 0{\cdot}7$	$(H = h_1 + h_2)$

3.1 *Dispersion curves*

Dispersion curves for the cylinder of Table 1 appear in Figs. 1 and 2. In both graphs, the abscissa is nondimensional wave number $\Delta = kH$. In Fig. 1 the ordinate is nondimensional phase velocity $s = c/\beta^* = \omega/k\beta^*$, and in Fig. 2 it is nondimensional frequency $\Omega = \omega H/\beta^*$. The reference velocity $\beta^* = (\beta_1 + \beta_2)/2$.

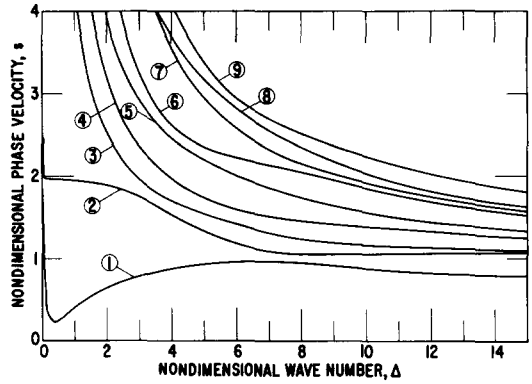

FIG. 1. Phase velocity vs. wave number.

The approach of the phase velocity to various limiting values may be examined in Fig. 1. For instance, for very long waves, the phase velocity of the first mode approximates that of "bar" waves. Also, for very short waves the phase velocity of the first mode approaches the Rayleigh wave speed of the slower medium. The occurrence in this first mode curve of a relative maximum value of phase velocity for an intermediate value of wave number would appear to be unique to layered media.

For the second and higher modes the phase velocity becomes very large as the wave number is made smaller. Therefore, the long wavelength behavior of these modes is better examined in the frequency wave number plot of Fig. 2. In Fig. 2 it is observed that curves for all the modes except the first have a finite frequency intercept for zero wave number. These frequencies and the character of the motion for each of the modes are summarized in Table 2. Other features of the curves presented in Fig. 2 include the relative minimum

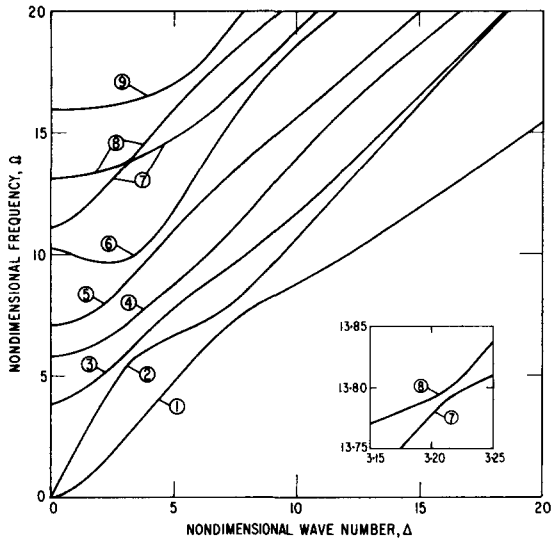

FIG. 2. Frequency vs. wave number.

TABLE 2. CHARACTER OF THE INFINITE WAVELENGTH AXIALLY SYMMETRIC VIBRATIONS OF THE TWO-LAYERED CYLINDER OF TABLE 1

Mode	Frequency, Ω	Character of motion
1	0	zero nodes, axial motion
2	0·066	zero nodes, radial motion, "ring" vibration
3	3·86	1 node, axial motion, thickness shear
4	5·80	2 nodes, axial motion, thickness shear
5	7·07	1 node, radial motion, thickness stretch
6	10·2	3 nodes, axial motion, thickness shear
7	11·1	2 nodes, radial motion, thickness stretch
8	13·1	4 nodes, axial motion, thickness shear
9	15·9	5 nodes, axial motion, thickness shear

of mode 6 near $\Delta = 2{\cdot}5$ (this corresponds to zero group velocity) and the close approach of modes 7 and 8 near $\Delta = 3{\cdot}1$. The inset of Fig. 2 shows this close approach on a magnified scale.

3.2 *Displacements*

Displacements and stresses (see next section) are seldom presented. While they were originally calculated to assess the approximate shell theory of Ref. [1], they are of interest *per se*. They are calculated for wave lengths and frequencies well outside the range of any shell theory and thus provide a valuable insight into the development of the breakdown of the assumptions of thin shell theory. It is felt that this is a unique feature of the present work.

In [1] an approximate shell theory is developed and partially compared with the present exact solutions. Figures 3–7 extend the comparison of displacements over the entire range of interest. Due to the eigenvalue nature of the problem considered, the absolute magnitudes of the displacements are undetermined since multiplication by a constant (normalization)

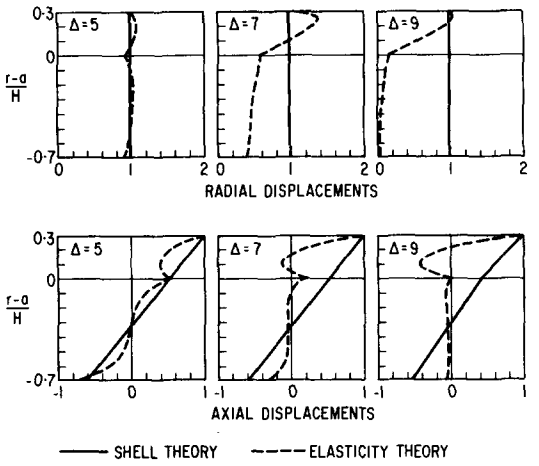

FIG. 3. First mode displacement distributions.

factor is permissible. Therefore, our comparisons are of the shapes of the displacement distributions, the magnitude having been adjusted to make the present exact theory and the shell theory of [1] agree at some convenient value of r. Solution for both theories of a forced motion problem would permit comparisons of magnitudes as well. However, examination of the shapes alone of the displacement distributions is of interest since formulations of higher order shell theories generally postulate functional forms for the dependence of the displacements on the thickness coordinate.

For the present comparisons the axial displacements have been normalized to make exact theory and shell theory displacements equal to one at the outer surface. This normalization, of course, fixes definite ratios between the radial displacements of the two theories at every location in the shell (except in the case of infinite wavelength where axial and radial motion are uncoupled). The radial displacements need nowhere be equal. Rather than present them in such a form we have taken the liberty of introducing a different normalization of the radial displacements. The radial displacements from both theories are made equal to one at the outer surface. Such a normalization is necessary for uncoupled radial motion, and moreover it permits the use of a uniform scale for nearly all the radial displacement plots. The information suppressed by this normalization convention, that is, the ratio of the maximum outer surface radial displacement to maximum outer surface axial displacement, is presented in Table 3.

In [1] the first mode axial and radial displacements (as well as the dispersion curves) were compared for a limited range of $\Delta < 3{\cdot}0$. Figure 3 extends this comparison up to $\Delta = 9{\cdot}0$. Since several curves for $0 < \Delta \leq 3{\cdot}0$ were presented in Ref. [1], the curves in Fig. 3 start at $\Delta = 5{\cdot}0$. Further, for $\Delta < 3{\cdot}0$, there is little variation of radial displacement through the thickness, and the axial displacement differs little from the bi-linear distribution assumed in the shell theory. Starting at $\Delta = 5{\cdot}0$ the nonuniformity of radial displacement begins to become pronounced, and the axial displacement becomes increasingly nonlinear.

Previous analyses [1, 21] show that as the wave number becomes increasingly large the first mode decays from a flexural mode into a Rayleigh wave in the slower medium. It is apparent in the curves for $\Delta = 9{\cdot}0$ that this transition is nearly complete: the motion is

TABLE 3. RATIOS OF OUTER SURFACE MAXIMUM RADIAL DISPLACEMENT TO OUTER SURFACE MAXIMUM AXIAL DISPLACEMENT

Mode	Wave number, Δ	Displacement ratio	
		Exact theory	Shell theory
	5	1·089	1·370
1	7	1·460	1·531
	9	1·630	1·739
	0	∞	∞
2	1	−0·277	−0·0165
	3	−2·621	−0·045
	0	0	0
3	1	−0·1025	−0·0467
	3	−0·0428	−0·0521
	0	0	0
4	1	0·522	0·0277
	3	1·886	0·0962
	0	∞	—
5	1	−11·96	—
	3	−21·50	—

concentrated almost entirely in the outer medium. One might expect certain of the displacement plots to exhibit other surface or interface waves. However, with the parameters used for these two media, calculations show that Stoneley waves do not exist at the interface ([19], p. 113). Theory predicts that for sufficiently high wave numbers a Rayleigh wave will form in the faster (inner) medium. Such a wave is manifested in a more complicated way called "terracing," [22] and its consideration would require investigation of a larger range of Δ than has been undertaken for the present work.

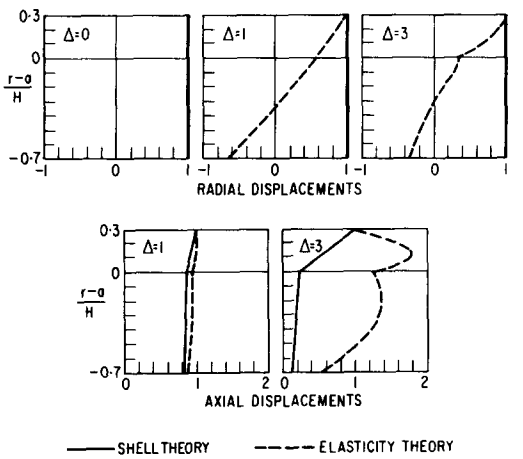

FIG. 4. Second mode displacement distributions.

Figure 4 shows the second mode displacements for Δ = 0, 1, and 3. For Δ = 0, the motion is totally radial, and no plot of axial displacements is necessary. In contrast to the first mode, the displacement curves degenerate from the shell theory quite rapidly with a

phase reversal in the radial displacement already apparent at $\Delta = 1{\cdot}0$. By $\Delta = 3{\cdot}0$ the nonlinearity of the curves is pronounced. They are totally different from those of the shell theory. The radial displacement curves for both $\Delta = 1{\cdot}0$ and $3{\cdot}0$ are evidence that considerable thickness-stretch deformation is present.

Figures 5 and 6 show the displacements for the third and fourth modes. They are predominantly thickness-shear modes. At $\Delta = 0$ the motion is purely axial; therefore no radial

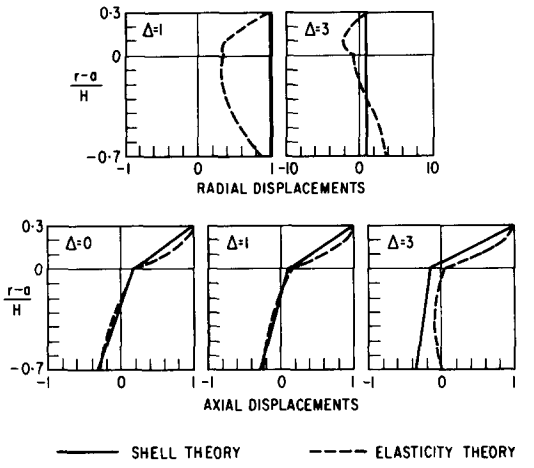

FIG. 5. Third mode displacement distributions.

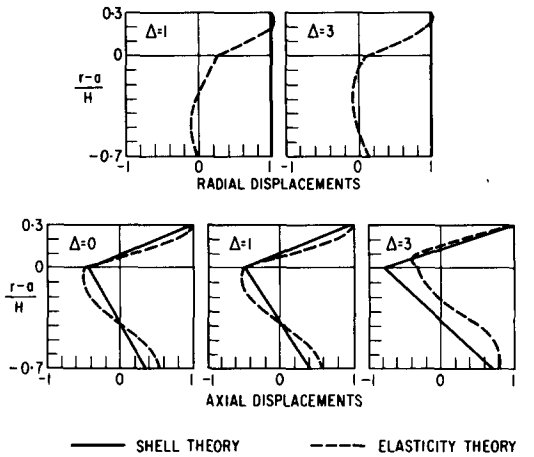

FIG. 6. Fourth mode displacement distributions.

displacement plots appear. In both figures, the predictions from shell theory compare quite well with the exact solution, at least for the axial displacements. As in the second mode there is sufficient thickness-stretch motion present to cause the appearance of nodes in most of the radial displacement plots. Note in Fig. 5 that the radial displacements for $\Delta = 3$ are plotted to a different scale than the rest.

Figure 7 shows the displacements for the fifth mode, the first mode not predicted by shell theory. At $\Delta = 0$ the motion is purely radial or thickness-stretch. At least for small

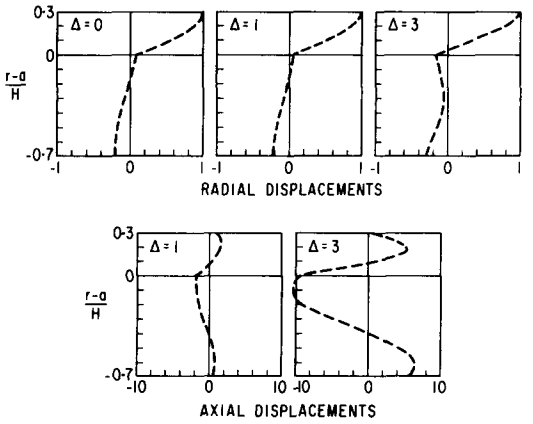

FIG. 7. Fifth mode displacement distributions.

wave number the shapes of the radial displacement curves are such that a linear distribution might offer a good approximation. Thus, a higher order shell theory admitting a linear distribution of radial displacements might give fair results for the long wavelength portion of the fifth mode. Such a shell theory has been presented by Mirsky [23] for a single-layer cylindrical shell. Resuming the examination of Fig. 7 one sees that for finite wave numbers axial motion is present in a form that resembles double-node thickness shear. However, the axial motion shows little tendency toward linearity, indicating that (the same as in the lower modes) a shell theory with linear axial displacement variation through the thickness will probably not give a reasonable approximation for larger wave numbers.

In summary the comparisons of the displacements for the four lowest modes shows that the second mode yields the poorest comparison between exact and shell theory. Although this result is surprising, it could have been anticipated since the second mode dispersion curve deviates more from that predicted by shell theory for lower values of Δ than for the other modes. It would appear that the incorporation of thickness-stretch deformations is the next essential step in improving the shell theory for high frequency, short wavelength use.

3.3 *Stresses*

Figures 8–11 describe the axial stress (σ_{zz}) and the shear stress (σ_{rz}) distributions. As with the displacements the absolute magnitude of the stresses cannot be determined. The stresses from both the exact and shell theories were normalized so that the greatest axial stress at the outer edges or at the interface was set equal to either $\pm 1{\cdot}0$. This also fixes the magnitudes of the shear stresses.

Figures 8 and 9 show, respectively, the first mode axial and shear stresses. It is seen in Fig. 8 that for $\Delta \leq 3$ there is good agreement with the shell theory. However, as Δ increases the agreement deteriorates. By $\Delta = 7$ there is only fair agreement, and by $\Delta = 9$ there is almost none. The latter point is confirmed by the previous observation that by $\Delta = 9$ there is a Rayleigh wave formed in the outer medium. Figure 9 is probably of more interest since

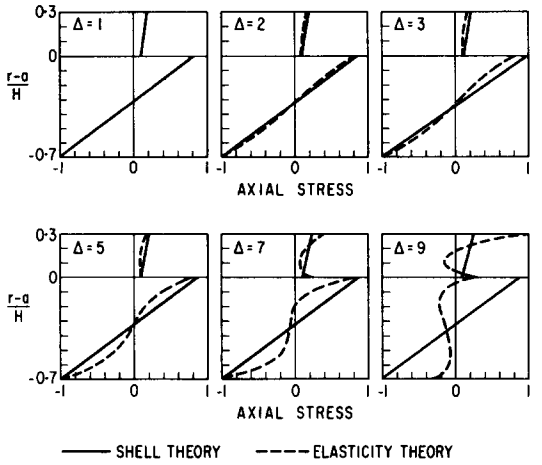

FIG. 8. First mode axial stress distributions.

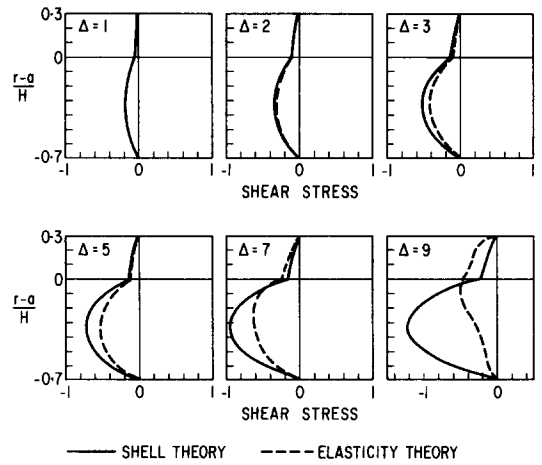

FIG. 9. First mode shear stress distributions.

an expected mode of failure of multilayered shells is in shear failure of the bond. The shear stress distribution follows roughly the same pattern as the axial stresses, being close to the shell theory for $\Delta \leq 5$ and being totally different by $\Delta = 9$.

Figure 10 shows the second mode stresses. As might be expected there is not as good an agreement as with the first mode. By $\Delta = 3{\cdot}0$ the shell theory stress distributions are beginning to diverge sharply from the exact ones.

Figure 11 shows third mode stress distributions. There is good agreement with shell theory only for $\Delta \leq 1$. By $\Delta = 2$ there is considerable divergence in the stresses, and by $\Delta = 3$ the exact theory curves bear little resemblance in shape to those from the shell theory. The fourth mode curves, while not presented, show a pattern similar to the third mode. It is worth noting that although the stress comparison plots are useful for illustrating qualitative differences between the theories the quantitative interpretation can be quite sensitive to the particular normalization convention that is adopted.

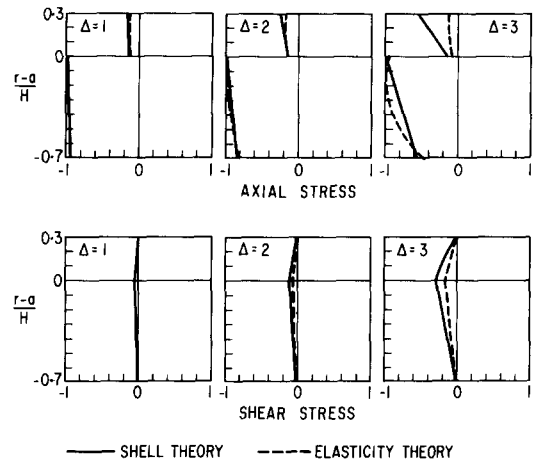

FIG. 10. Second mode stress distributions.

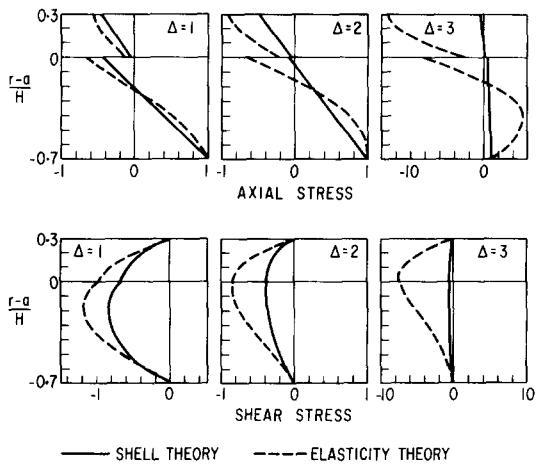

FIG. 11. Third mode stress distributions.

In conclusion it is felt that if any shell theory is to be improved by the introduction of more dependent variables, thickness-stretch motion is essential. For still higher modes to yield agreement it would be necessary to add additional shear deformations corresponding to warping of initially plane cross sections.

4. CONCLUSIONS

The observations presented here on the dynamics of a two-layered cylinder are specifically pertinent to axially symmetric motions of a relatively thin-walled cylinder. The equations, however, are in no way restricted to shell-like geometry. The observations are also pertinent to the shell theory of [1] insofar as it is in agreement with the exact theory.

In many respects the results are similar to those for a homogeneous hollow cylinder.

In the lowest mode very long waves propagate with a finite phase velocity. (To the scale used in Fig. 1 this may not be immediately evident). Infinite wavelength vibrations in the second mode occur with a finite cutoff frequency corresponding to purely radial vibrations of the cylinder. Cutoff frequencies for the higher modes correspond to simple thickness-shear or thickness-stretch vibrations. For small enough wavelengths and/or for the higher modes a good description of the motion is obtained using the simpler equations for the propagation of straight crested waves in a plane medium of the same thickness.

However, unlike a homogeneous hollow cylinder a two-layered cylinder does not have equal surface wave velocities at its inner and outer surfaces. When the slower layer is much thinner this leads to a relative maximum at intermediate wavelength of the first mode phase velocity vs. wave number curve. For larger wave numbers the phase velocity is decreasing, and it thus approaches from above the Rayleigh wave velocity of the slower medium. This character of the phase velocity dispersion relation is not matched even qualitatively by a Timoshenko-type shell theory. Presumably duplication of this behavior would require a higher order shell theory accommodating cross section distortions such that initially plane cross sections of either layer no longer remain plane in the deformed shell.

Some further conclusions pertinent to the development of higher order shell theories are in order. The displacement and stress distributions presented here reinforce the conclusion that good results are obtained by incorporating shear deformation individually in each layer such as was done in [1]. Also it appears that if one desired to extend the range of applicability of the theory of [1] by adding more dependent variables, the next logical step would be incorporation of thickness-stretch deformation individually in each layer.

Acknowledgements—Numerical computations for this paper were carried out on a digital computer at the Aerospace Corporation Computing Center. Programming was accomplished by Mrs. H. S. Porjes, with analytical consultation furnished by R. Duty. Their fine assistance is gratefully acknowledged. Likewise, the authors are indebted to Mrs. E. F. Farkas for her assistance with hand computations of check cases and to Mrs. J. Burris for assistance in manuscript preparation.

REFERENCES

[1] J. P. JONES and J. S. WHITTIER, *J. appl. Mech.* **33**, 838 (1966).
[2] L. POCHHAMMER, *J. reine angew. Math.* **81**, 324 (1876).
[3] C. CHREE, *Trans. Camb. phil. Soc.* **14**, 250 (1889).
[4] J. GHOSH, *Bull. Calcutta math. Soc.* **14**, 31 (1923).
[5] D. C. GAZIS, *J. acoust. Soc. Am.* **30**, 786 (1958).
[6] D. C. GAZIS, *J. acoust. Soc. Am.* **31**, 568 (1959).
[7] D. C. GAZIS, *J. acoust. Soc. Am.* **31**, 573 (1959).
[8] J. E. GREENSPON, *J. acoust. Soc. Am.* **31**, 1682 (1959).
[9] J. E. GREENSPON, *J. acoust. Soc. Am.* **32**, 571 (1960).
[10] G. HERRMANN and I. MIRSKY, *J. appl. Mech.* **23**, 563 (1956).
[11] I. MIRSKY and G. HERRMANN, *J. acoust. Soc. Am.* **29**, 1116 (1957).
[12] I. MIRSKY and G. HERRMANN, *J. appl. Mech.* **25**, 97 (1958).
[13] P. M. NAGHDI and R. M. COOPER, *J. acoust. Soc. Am.* **28**, 56 (1956).
[14] R. M. COOPER and P. M. NAGHDI, *J. acoust. Soc. Am.* **29**, 1365 (1957).
[15] J. F. BIRD, *J. acoust. Soc. Am.* **32**, 1413 (1960).
[16] J. F. BIRD, R. W. HART, and F. T. MCCLURE, *J. acoust. Soc. Am.* **32**, 1404 (1960).
[17] J. H. BALTRUKONIS, W. G. GOTTENBERG, and R. N. SCHREINER, *J. acoust. Soc. Am.* **33**, 1447 (1961).
[18] H. D. MCNIVEN, J. L. SACKMAN, and A. H. SHAH, *J. acoust. Soc. Am.* **35**, 1602 (1963).
[19] W. M. EWING, W. S. JARDETSKY, and F. PRESS, *Elastic Waves in Layered Media*. McGraw-Hill (1957).
[20] H. SAITO and K. SATO, *J. appl. Mech.* **29**, 287 (1962).
[21] J. P. JONES, *J. appl. Mech.* **31**, 213 (1964).

[22] R. D. MINDLIN, *An Introduction to the Mathematical Theory of Vibrations of Elastic Plates*, prepared for U.S. Army Signal Corps Engineering Laboratories, Fort Monmouth, N.J., Signal Corps Project 142B (1955).
[23] I. MIRSKY, *J. acoust. Soc. Am.* **36**, 41 (1964).
[24] W. MAGNUS and F. OBERHETTINGER, *Special Functions of Mathematical Physics*. Chelsea Publ. Co. (1949).

APPENDIX

EXPRESSIONS FOR BOUNDARY CONDITIONS

Equations resulting from the satisfaction of free surface and interface boundary conditions, equations (15), appear in this Appendix; they are:

$$A_1P_{11}+B_1Q_{11}+C_1R_{11}+D_1S_{11}=0 \tag{A1}$$

$$A_1T_{11}-B_1U_{11}+C_1V_{11}-D_1W_{11}=0 \tag{A2}$$

$$\begin{aligned}A_1\mu_1P_{10}+B_1\mu_1Q_{10}+C_1\mu_1R_{10}+D_1\mu_1S_{10}\\ =A_2\mu_2P_{20}+B_2\mu_2Q_{20}+C_2\mu_2R_{20}+D_2\mu_2S_{20}\end{aligned} \tag{A3}$$

$$\begin{aligned}A_1\mu_1T_{10}-B_1\mu_1U_{10}+C_1\mu_1V_{10}-D_1\mu_1W_{10}\\ =A_2\mu_2T_{20}-B_2\mu_2U_{20}+C_2\mu_2V_{20}-D_2\mu_2W_{20}\end{aligned} \tag{A4}$$

$$\begin{aligned}A_1\varepsilon_1I_1(k\varepsilon_1a)-B_1\varepsilon_1K_1(k\varepsilon_1a)+C_1\delta_1I_1(k\delta_1a)-D_1\delta_1K_1(k\delta_1a)\\ =A_2\varepsilon_2I_2(k\varepsilon_2a)-B_2\varepsilon_2K_1(k\varepsilon_2a)+C_2\delta_2I_1(k\delta_2a)-D_2\delta_2K_1(k\delta_2a)\end{aligned} \tag{A5}$$

$$\begin{aligned}A_1I_0(k\varepsilon_1a)+B_1K_0(k\varepsilon_1a)+C_1\delta_1^2I_0(k\delta_1a)+D_1\delta_1^2K_0(k\delta_1a)\\ =A_2I_0(k\varepsilon_2a)+B_2K_0(k\varepsilon_2a)+C_2\delta_2^2I_0(k\delta_2a)+D_2\delta_2^2K_0(k\delta_2a)\end{aligned} \tag{A6}$$

$$A_{22}P_{22}+B_2Q_{22}+C_2R_{22}+D_2S_{22}=0 \tag{A7}$$

$$A_2T_{22}-B_2U_{22}+C_2V_{22}-D_2W_{22}=0 \tag{A8}$$

where the lengthier combinations of Bessel functions have been abbreviated according to the following

$$\left.\begin{aligned}P_{ij}&=(1+\delta_i^2)I_0(k\varepsilon_ia)-2\varepsilon_i^2\frac{I_1(k\varepsilon_ia)}{k\varepsilon_ia}\\ Q_{ij}&=(1+\delta_i^2)K_0(k\varepsilon_ia)+2\varepsilon_i^2\frac{K_1(k\varepsilon_ia)}{k\varepsilon_ia}\\ R_{ij}&=2\delta_i^2\left[I_0(k\delta_ia)-\frac{I_1(k\delta_ia)}{k\delta_ia}\right]\\ S_{ij}&=2\delta_i^2\left[K_0(k\delta_ia)+\frac{K_1(k\delta_ia)}{k\delta_ia}\right]\\ T_{ij}&=2\varepsilon_iI_1(k\varepsilon_ia)\\ U_{ij}&=2\varepsilon_iK_1(k\varepsilon_ia)\\ V_{ij}&=\delta_i(1+\delta_i^2)I_1(k\delta_ia)\\ W_{ij}&=\delta_i(1+\delta_i^2)K_1(k\delta_ia)\end{aligned}\right\} \tag{A9}$$

where i takes on values 1 and 2. The subscript j takes on values 1, 0, and 2, which corresponds to multiplying the arguments by $1+\lambda_1$, 1, and $1-\lambda_2$, respectively; e.g.

$$P_{il} = (1+\delta_i^2)I_0[k\varepsilon_i a(1+\lambda_1)] - 2\varepsilon_i^2 \frac{I_1[k\varepsilon_i\mu(1+\lambda_1)]}{k\varepsilon_i\mu(1+\lambda_1)}, \text{ etc.}$$

Here $\lambda_1 = (h_1/a)$ and $\lambda_2 = (h_2/a)$.

(*Received* 13 *May* 1966; *revised* 3 *October* 1966)

Résumé—La théorie linéaire d'élasticité est employée pour investiguer des propagations d'ondes axialement symmetriques dans un cylindre à deux couches d'une longueur infinie. Chaque matière est supposée être homogène et isotrope. Un lien parfait est assumé à l'interface alors que les limites intérieures et extérieures du cylindre composite sont traîtées comme libres de traction. Le déterminant de dispersion relatant la vélocité de phase et le nombre d'ondes pour un train d'ondes harmoniques satisfaisant ces conditions de limite est présenté. Le caractère de l'équation de dispersion est investigué analytiquement et numériquement. Les distributions de contrainte et de déplacement sont également présentées pour l'exemple numérique. Des comparisons sont faites avec une solution approximative du méme problème obtenue au moyen d'une théorie de couche fine incorporant une déformation de cisaillement-épaisseur de chaque couche.

Zusammenfassung—Die lineare Elastizitätstheorie wird angewandt zur Untersuchung der drehsymmetrischen Wellen-Ausbreitung in einem doppelschichtig unendlichen Zylinder. Jedes Material wird als homogen und isotrop vorausgesetzt. Tadellose Verbindungen der Grenzflächen werden vorausgesetzt; während die inneren und äusseren Grenzen des zusammengesetzten Zylinders als kraftfrei behandelt werden. Die Streuungs-Determinante, die Phasengeschwindigkeit und Wellennummer einer harmonischen Wellenreihe darstellt und die Grenzbedingungen erfüllt wird gegeben. Die Streuungsgleichung wird analytisch und numerisch untersucht. Die Verteilung von Spannung und Verschiebung werden auch gegeben, für das numerische Beispiel. Die Resultate werden mit den Resultaten verglichen die erhalten werden wenn man die Dünnwandtheorie anwendet und die Verformungen durch Dicke-Scherung berücksichtigt.

Абстракт—Применяется линейная теория эластичности для исследования симметрического относительно оси распространения волны в бесконечно длинном двуслойном цилиндре. Считается, что каждый материал гомогенен и изотропен. Связь у поверхности раздела принимается, как идеальная, в то время, как внутренние и внешние линии раздела составного цилиндра считаются лишёнными сил сцепления. Даётся определитель рассеяния скорости относительной фазы и число волны для гармонического состава волн, удовлетворяющих этим граничным условиям. Характер уравнения рассеяния исследуется аналитически и численно. Для численного примера даются также распределения напряжения и смещения. Сделаны сравнения с приблизительным решением той же самой проблемы, полученным посредством теории тонкой оболочки, включающей деформацию толщины-сдвига каждого слоя.